GOLF: A RESONANCE SPECTROMETER FOR THE OBSERVATION OF SOLAR OSCILLATIONS

II) EXPERIMENTAL TESTS OF THE CELL RESPONSE

BOUMIER P. [1], DECAUDIN M. [1], JONES A.R. [2], GREC G. [3], TAMIATTO C. [1]

1 Institut d'Astrophysique Spatiale, bât. 121, Université Paris XI, 91405 Orsay Cedex, France.

2 Kapteyn Sterrenswacht, Mensingheweg 20, 9301 KA, Roden, The Netherlands.

3 Département d'Astrophysique, Université de Nice, France.

(Received 6 May 1993; accepted 16 December 1993)

ABSTRACT

GOLF (Global Oscillations at Low Frequencies) is an instrument to study the line-of-sight velocity of the solar photosphere, to be flown on the SOHO satellite in 1995. It uses a sodium vapour cell in resonance scattering mode, in order to measure the absolute Doppler shift of the solar sodium absorption lines. We detail laboratory tests to determine the performances of the cell built for the experiment. The results are in good agreement with numerical simulations of the resonance processes. As a final result, we can conclude that the level of performances required for the flight instrument will be obtained.

I INTRODUCTION

Helioseismology is the study of global oscillations of the Sun. These oscillations are of very low amplitude and thus require very sensitive instruments to study them. However, the knowledge gained by this study is well worth the effort, as the oscillations probe the depth of the Sun, and provide a window into the solar interior. One way to measure the oscillations is to record the solar surface velocity. The technique of resonance spectroscopy was one of the first used in this endeavour (Brookes et al, 1978; Fossat and Roddier 1971). Since that time, solar oscillations have been extensively studied from the ground, and there have also been measurements from space by the SMM mission (Woodard and Hudson 1983; Woodard 1987), and the very successful IPHIR experiment on the PHOBOS satellites (Fröhlich et al, 1988a and 1991; Toutain and Fröhlich1992). In the future, a joint venture of ESA and NASA will provide a stable platform viewing the Sun for at least two years starting in 1995: SOHO (SOlar and Heliospheric Observatory). SOHO will carry three experiments dedicated to helioseismology:

- VIRGO (Variability of IRradiance and Gravity Oscillations; Fröhlich et al, 1988b) is a package containing 4 photometers (one providing low resolution of the solar disc) and two independent radiometers.
- SOI (Solar Oscillation Investigation; Scherrer et al, 1991) provides very high spatial resolution of the solar disc, and will give both velocity and magnetic field maps of the Sun.
- GOLF (Global Oscillations at Low Frequencies) is a natural extension of the ground based resonant scattering instruments modified for use in space. The principle of GOLF was described in detail by Damé et al (1987), Gabriel et al (1991) and more recently by Boumier and Damé (1993). Briefly, it consists of determining the velocity of the solar photospheric layers, by measuring the Doppler shift of the sodium Fraunhofer lines (5896 and 5890 Å). The technique used is resonance spectrometry,

Experimental Astronomy **4**: 237–252, 1994.

which offers extremely high stability and spectral resolution. In this paper, we present some experimental tests of the resonance characteristics, and we compare them with the predictions of a numerical model (Boumier 1991; Boumier and Damé 1993).

II EXPERIMENTAL SETUP

All the experiments were performed using the facilities of the Institut d'Astrophysique Spatiale d'Orsay (IAS). The resonance cell and the magnet used are GOLF prototypes: the cell has an internal length of 15 mm and an internal diameter of 10 mm; the magnetic field at the center of the cell is about 5050 Gauss (higher than the original design value of 4750 Gauss). A vacuum tank (pressure between 10^{-6} and 10^{-7} mm Hg) produces the space-like environment required to operate the sodium cell, due to the multi-layer insulation and the heating devices used: the experimental settings are as similar as possible to the flight model, in order to provide realistic measurements for both the optical and thermal properties.

The instrumental setup is shown Figure 1. The cell-magnet system is mounted on a three-axis mount, so that it can be centered and rotated around the vertical, as necessary. The optical layout is identical to GOLF: the entrance pupil (L1) is reimaged by the lens L2 at the center of the cell. The linear polarizer and the quarter-wave plate are mounted on independently rotating devices, allowing the polarization of the beam entering the cell to be chosen at will. The relative position of the axis of the two components is determined to within 0.02°.

The light source, either a Xenon lamp to simulate the solar continuum, or a tuneable dye laser, is focused on an optical fiber connected to the vacuum tank. The laser has a spectral width of about 0.01 mÅ at 5890 Å. The wavelength can be scanned so that the spectral properties of the resonance can be investigated. During a scan, part of the laser beam passes through an iodine vapour to provide wavelength calibration. When using the Xenon lamp, a 20 Å FWHM interference filter with the same spectral characteristics as the GOLF filter is placed in front of L1 to define the optical bandwidth.

Two signals are recorded: the resonantly scattered light (which GOLF will measure), and referred to as the resonance signal, and the light transmitted through the cell. The detectors used are Hamamatsu S20 photomultipliers operated in the photon counting mode; these tubes and associated electronics are similar to the flight versions.

The temperature of the cell stem is a critical parameter of the measurements, as it is this which determines the sodium vapour pressure. The temperature is servo controlled using the measured value to control the current supplied to the stem heater. The head of the cell is maintained hotter than the stem by a constant current fed to the head heater. The temperatures are recorded with an accuracy of 0.25 °C and 0.005 °C for the head and stem respectively, using a thermo-couple for the head and a platinium resistance thermometer for the stem. For the optical study, one has to keep in mind an additional point due to mechanical constraints: the thermal study shows that if the insulating layers do not achieve a sufficient efficiency, the non-cylindrical part at the end of the stem will be cooler than the temperature-controlled part, leading to a sodium vapour pressure lower than expected from the temperature reading of the platinium probe.

III BROAD BAND MEASUREMENTS

Figure 2 shows the resonance signal normalized by the light transmitted through the cell*, with respect to the stem temperature. The signal reaches a maximum between 170 °C and 175 °C and decreases slowly at higher temperatures due to the increasing opacity of the vapour. It is hard to define the position of the maximum more precisely due to both measurement noise, and lack of precise knowledge of the vapour temperature. We will see below however, that for the

* Note that apart from normalization, the transmitted light allows us to check that there is no problem with the cell such as alignment errors or sodium deposits on the windows.

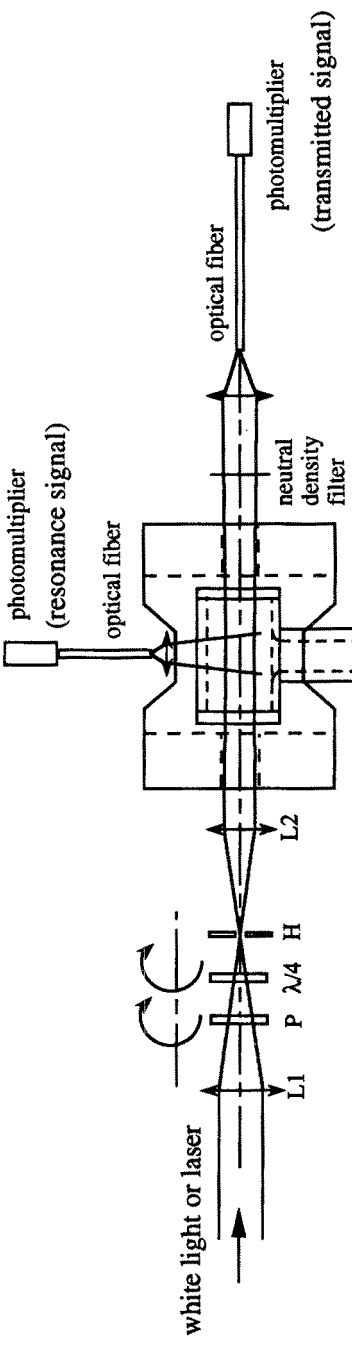

Figure 1: schematic setup for testing the GOLF resonance cell. The resonantly scattered light is measured by a system offset by 60° from the cell stem axis, in order to reduce the straylight contamination due to the joint between the head and the stem.

monochromatic measurements one can obtain a better estimate of the vapour temperature. The temperature giving the maximum flux is a few degrees higher than predicted by the resonance model. This difference is at least partly due to secondary resonance (resonance involving a photon coming from a first de-excitation) which has not been taken into account in the model; the effect of which is to compensate to some extent the loss in primary resonance at higher temperatures. This produces a flatter response with the maximum shifted a little to a higher temperature. The fraction of the resonantly scattered light which is collected is fully compatible with what was expected; this confirms that the counting rate expected for GOLF, and consequently the photon noise level, will be achieved.

From Figure 2 the signal to noise ratio (also called the resonance ratio) can be estimated. It is defined as the count rate from the resonance signal divided by the background signal. The latter is due to the photomultiplier's dark counts and from non-resonantly scattered light reaching the detectors. Measurements with the cell cold show that the latter dominates, contributing 70% of the background counts. We checked with the laser that this "cold" signal was not wavelength dependent, nor temperature dependent (setting the wavelength away from resonance and heating the cell). As far as the GOLF instrument is concerned, the value of the resonance ratio expected from our measurements is about 10. This rather low ratio comes from a high level of scattered light from the cell walls, and we hope to do better with new cells on which a special black enamel is deposited.

IV MONOCHROMATIC MEASUREMENTS

To understand in detail the performance of the instrument, one must study the spectral properties of the resonance signal. The laser can be set to scan over 30 GHz (i.e. over about 350 mÅ) near either the D1 or D2 lines of sodium. The duration of a scan is about 10 minutes, during which the resonance and transmission signals are measured simultaneously. A 1 second integration time is used corresponding to about a 0.6 mÅ spectral integration. Note that though the excitation is quasi monochromatic, the re-emitted light is not, but rather reflects the Doppler width of the atomic transitions in the vapour (about 20 mÅ). We are also not measuring purely the monochromatic profiles of the resonantly scattered light, but only a good estimation of them. A probable consequence is that the core of the real profiles is a little lower than measured.

Figure 3 shows the Zeeman transitions of the sodium doublet in the high field regime. The instrumental magnetic field is nominaly parallel to the optical axis, so that the π components should not be excited. As far as the σ components are concerned, the left circular polarized part of the incident beam excites the component shifted by the Zeeman effect towards the higher frequencies ($\sigma+$), the right circular polarized part exciting the one shifted towards the lower frequencies ($\sigma-$).

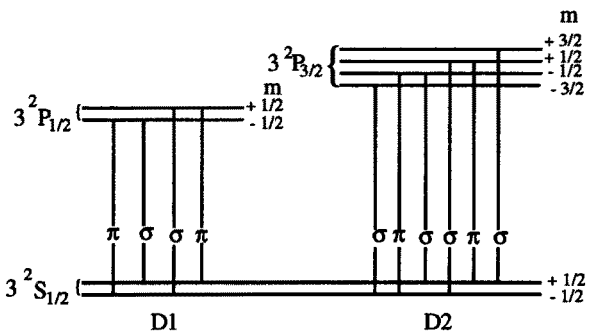

Figure 3: energy levels for sodium D lines

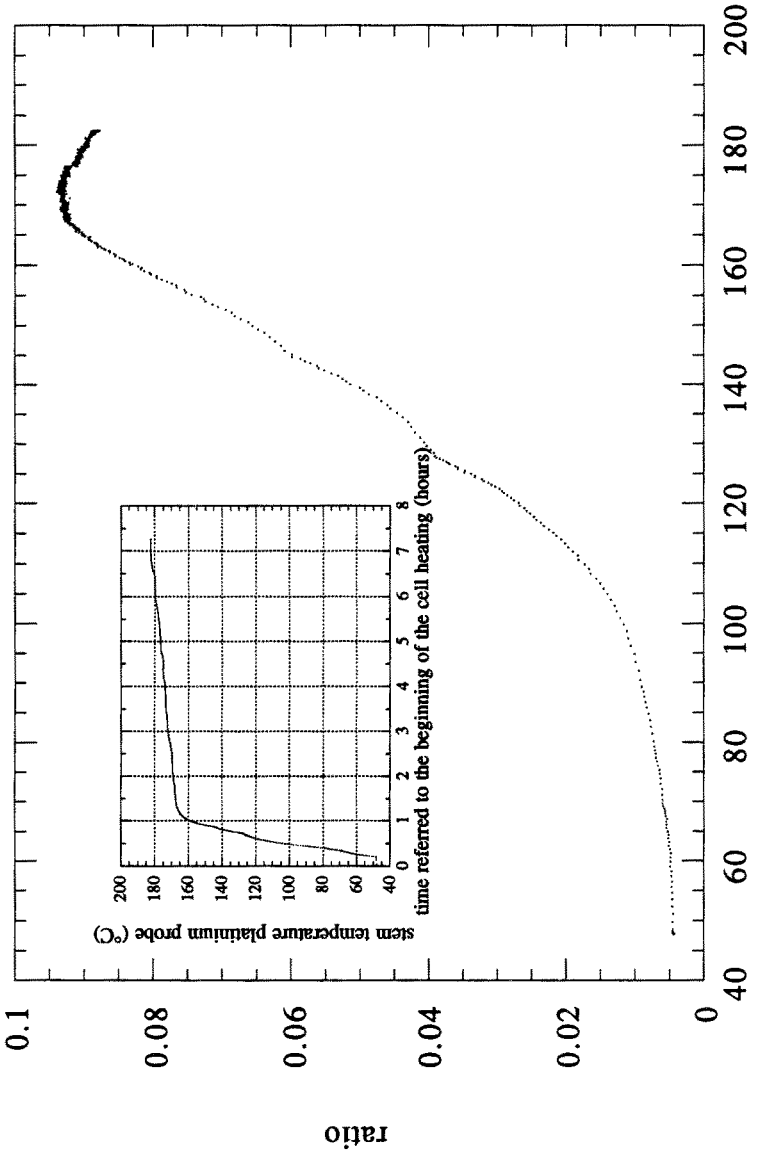

Figure 2: resonance signal / transmission signal: thermal sensitivity with white light source.

IV.1) Linear polarization at the entrance of the cell

To determine the solar radial velocity GOLF sequentially measures each side of the solar absorption line. This is accomplished by changing the circular polarization of the light entering the cell to excite only one of the σ component. However, it is useful to measure the resonance profiles with linearly polarized light. In this case, both σ components are excited, giving quasi symmetric profiles centered on their natural wavelengths. Figures 4 and 5 were obtained with a stem temperature of about 140 °C and the head close to 190 °C. The transmission curves show that the laser intensity can vary during a scan, and an interpolation was made for each scan to normalize the resonance signal.

From the transmission curve, it is possible to estimate the temperature of the liquid-vapour interface (inside the stem) by the determination of the absorption coefficients $k_{\sigma+}(\lambda)$ and $k_{\sigma-}(\lambda)$ relative to the circular states of polarization. We can write:

$$I_{tr}(\lambda) = I_{en}(\lambda)\,[\exp(-k_{\sigma+}(\lambda).L) + \exp(-k_{\sigma-}(\lambda).L)\,] / 2$$

$I_{tr}(\lambda)$ is the recorded transmission signal; $I_{en}(\lambda)$ is the entrance intensity (linearly polarized), estimated from the interpolation of the transmission signal off resonance; L is the internal length of the cell: 15 mm. The σ components are completly separated by the high magnetic field. This allows us to determine $k_{\sigma+}(\lambda)$ and $k_{\sigma-}(\lambda)$ independently. Then one can compare the absorption profiles with those of the model. The agreement between the σ components of both D1 and D2 lines leads to a precision of better than 1 °C for the vapour temperature. This correction of the platinium probe readings is exactly as predicted by the thermal modeling of the cell housing (Fourmond 1992).

What is not clearly visible in Figures 4.a and 5.a is that the π components are also excited and shifted. The excitation occurs because the magnetic field is not strictly parallel to the beam in the resonant volume, due to both the divergence of the beam (1°) and the non-uniformity of the magnetic field which increases towards the poles.

IV.2) Circular polarization at the entrance of the cell

Rotating the quarter-wave plate ±45° from the previous configuration, one can polarize the beam circularly (left or right). Figures 6 and 7 show the monochromatic efficiency of the cell ($T_{ce\lambda}$) obtained at different stem temperatures, plotted on a logarithmic scale. These figures correspond to the right circular polarization for the D1 scan, and left circular polarization for the D2 scan. The parameter $T_{ce\lambda}$ is defined as the ratio of the resonantly scattered light to the entrance light (Boumier 1991; Boumier and Damé 1993). The value of (λ_0) displayed on the figures has been calculated from the distance between the centroids of the peaks, below the saturation. The values determined agree with the accepted values (CRC Handbook of Chemistry and Physics) to within a few mÅ.

In addition to the desired σ peaks, residuals of the opposite σ as well as the π components are clearly visible. Note that the selection of a σ transition comes with the selection of the opposite π transition. The parasitic σ peaks can come first from the imperfect selection of the circular polarization and second from a depolarizing effect of the light when it traverses the cell glass. Further tests should help to determine which of these two processes dominates; if it is the first one, then the use of better polarizers and quarter-wave plates will improve the situation. The contribution of the parasitic peaks represents about 1% of the signal, which is 8 times less than the straylight scattered by the cell.

Saturation effects start to occur as the optical depth approaches unity, mainly due to absorption in the "non-seen" volume of the vapour. This is clearly seen in Figure 8. What the resonance model did not predict however was the asymmetry within the σ component, and moreover the maximum efficiency of the cell is wavelength dependent. We will see below that these two characteristics are linked, and due to the non uniformity of the magnetic field. However, a very encouraging result is

that the maximum efficiency is very close to the value of 7.6 10^{-4} predicted by the model. Note also that around the temperature giving the maximum flux (170 °C), the profiles are saturated, also predicted by the model. The core of the saturated profiles has an efficiency somewhat higher than in the model (~ 50 %). This departure can be due to the real geometry of the magnetic field (see next paragraph). On the other hand, we mentionned already the approximations of the model which does not include the thermal Doppler effect in the cell neither the secondary resonance (likely to contribute due to the relatively high opacity), leading to underestimate the efficiency in the core.

IV.3) Determination of the magnetic field in the resonating volume

In the case of a linearly polarized entrance beam, one can derive an estimate of the magnetic field in the vapour from the distance between the centroids of the σ components, below saturation. The mean value obtained for the three σ pairs is about 5100 Gauss. Another determination is also possible from the absorption coefficient profiles calculated from the transmission signal. This leads to the value of 5250 Gauss. The discrepancy between the two determinations is illustrated on Figure 9, for the D1 line profiles, for relatively low and high temperatures. The explanation was found in the fact that the two recorded signals do not correspond to a spatial integration over the same sodium volume, coupled with the non-uniformity of the magnetic field in the vapour (see Figure 10). The transmission signal results from absorption through the entire length of the cell (X axis), along which the gradient of the magnetic field is non-negligible. This signal corresponds also to an average absorption coefficient profile and consequently to an average value of the magnetic field which is significantly higher than the value at the center of the cell (5050 Gauss). On the other hand, the resonance signal comes from a smaller volume of vapour, close to the center of the cell. The average field seen by the detector is in that case only slightly different from the value at the center. To check this interpretation, a realistic magnetic field gradient, along the optical axis, has been introduced in the resonance model. The agreement with the measurements is excellent since the model correctly predicts the average magnetic field seen by a detector. Figure 11 shows a resonance profile as calculated by the new model. The asymmetry of the saturation is now present and is also produced by the heterogeneity of the magnetic field along the optical axis. It is due to the fact that the absorption of the light before the central volume where the resonance is seen, occurs at a relatively high magnetic field. This absorption, which is responsible for the saturation effect, also has a spectral profile shifted further from the natural wavelength than the profile of the light re-emitted in the central volume, that creates the asymmetry. Consequently, the efficiency of the cell ($T_{ce\lambda}$) becomes wavelength dependent, and its value is even closer to that predicted by the model. Note that the core of the calculated resonance profile is still lower than measured, for reasons already mentionned above.

The heterogeneity of the magnetic field has a practical consequence: the compromise between the absorption and the re-emission is less important, allowing us to heat the stem of the cell a little more than in the homogeneous field case. The broad band efficiency of the cell is also slightly increased. This suggests a design of what could be theoretically the "best" magnet for our kind of experiment, as far as the efficiency of the cell is concerned: a magnet with a constant field in the volume where the resonance is seen by the detector, and with a very different field elsewhere in order to separate as far as possible the absorption profiles not useful for us from the useful ones. The similar concept of multipole magnet has already been used in the ground-based MR5 resonance spectrometer experiment (Robillot et al, 1991), but for a different goal which is to measure simultaneously the intensity of 5 independent points regularly placed in the solar D1 sodium line.

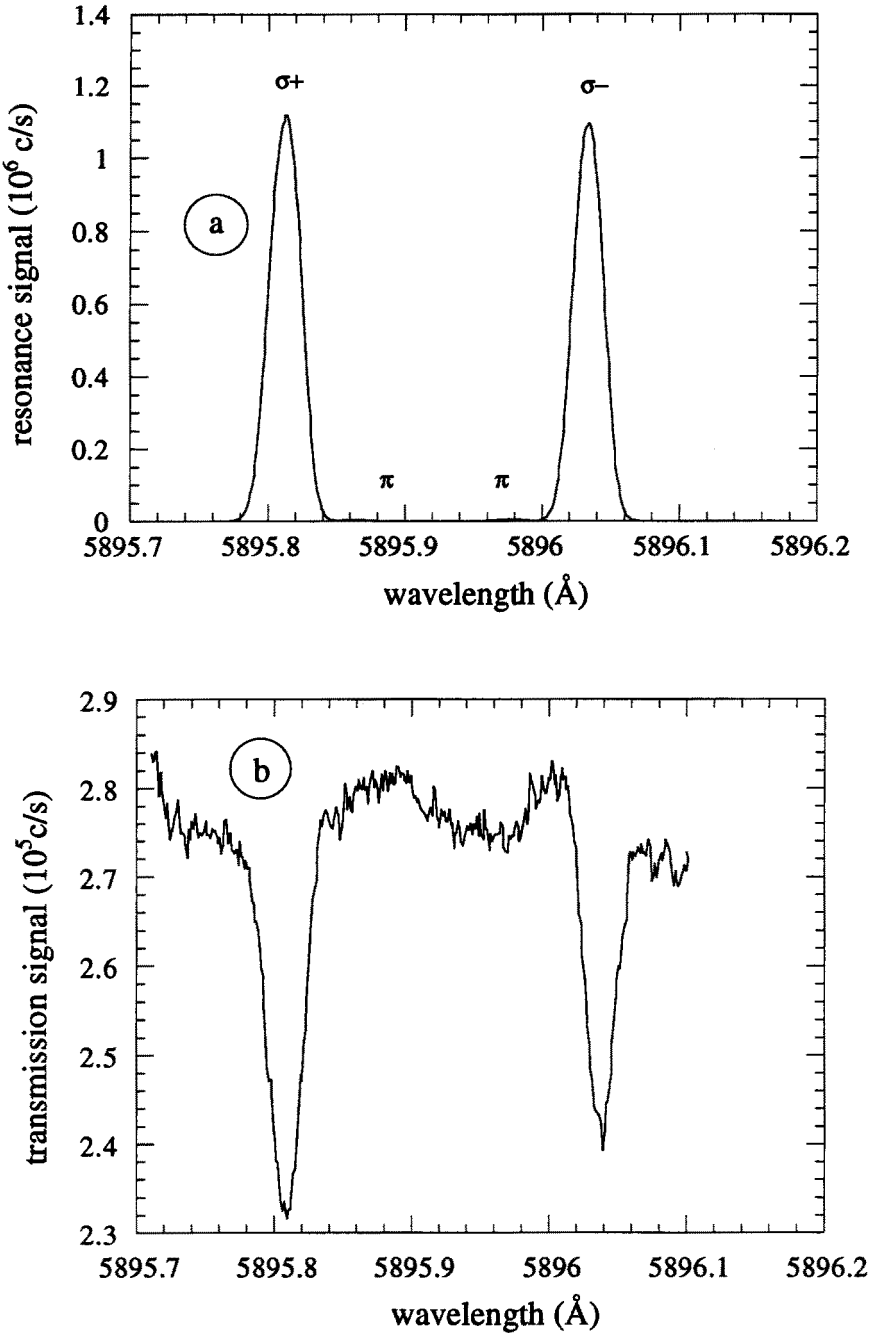

Figures 4: resonance (a) and transmission (b) signals for the D1 line, the incoming light being linearly polarized. Stem: 140°C; head: 190°C.

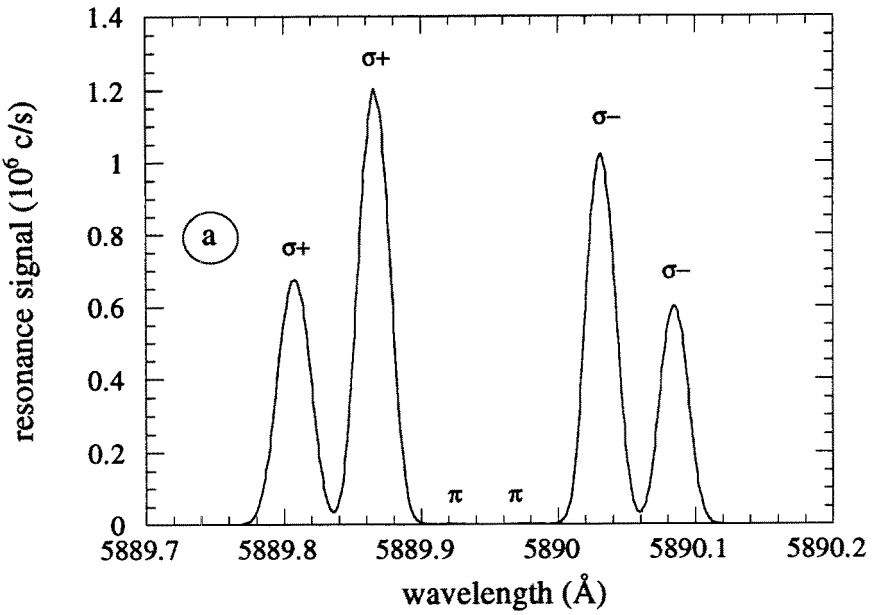

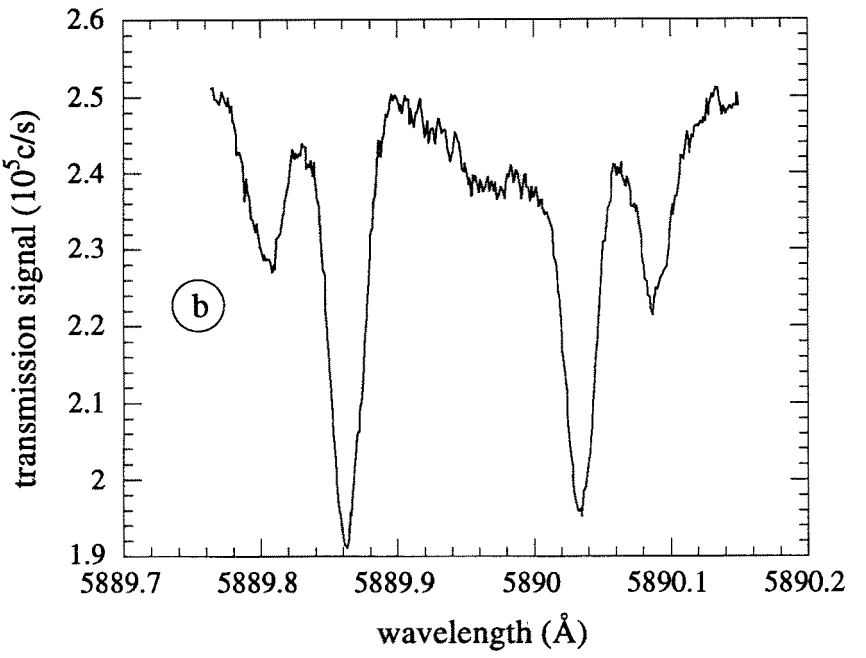

Figures 5: resonance (a) and transmission (b) signals for the D2 line, the incoming light being linearly polarized. Stem: 140°C; head: 190°C.

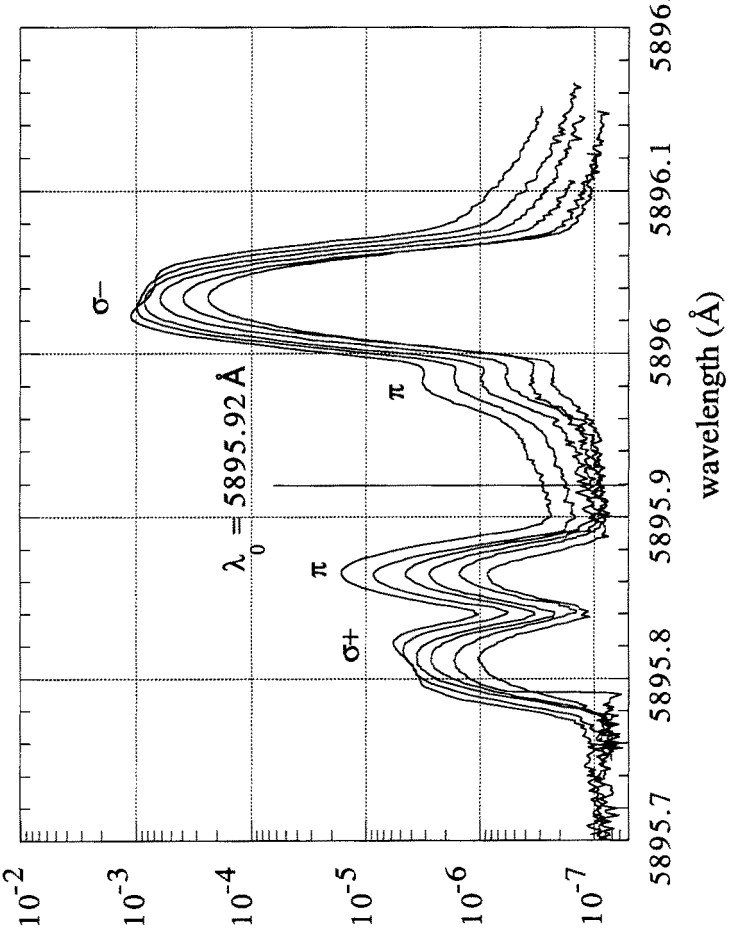

Figure 6: thermal properties of the monochromatic efficiency ($T_{ce\lambda}$) of the resonance cell (D1 line). stem temperatures: 130, 138, 146, 155, 163, 174 °C (head: 190 °C)

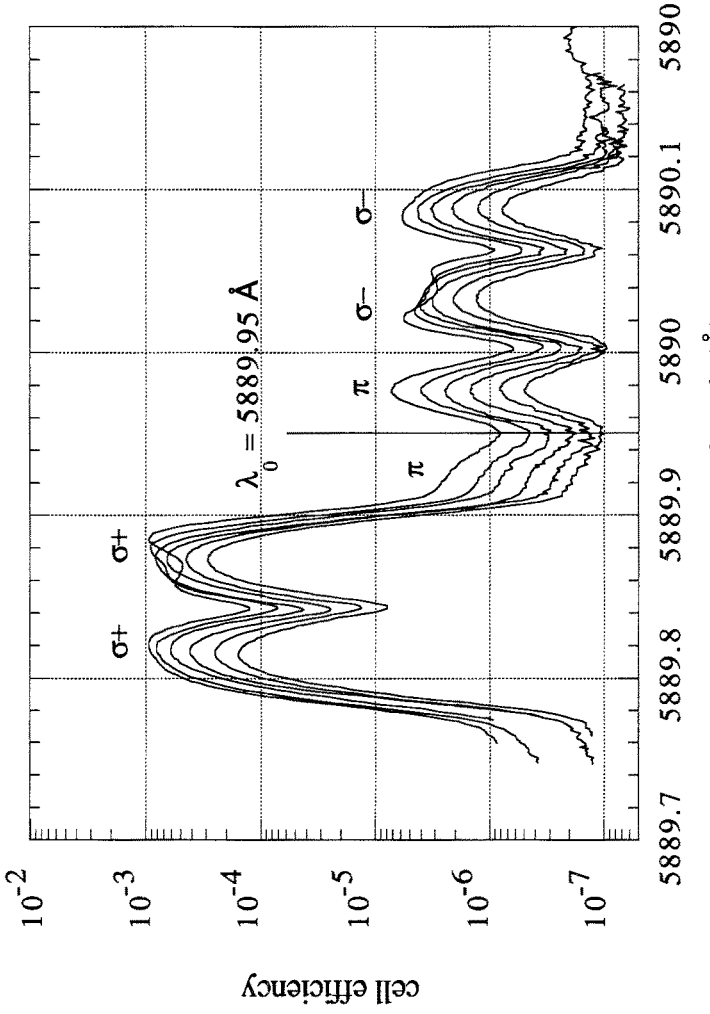

Figure 7: thermal properties of the monochromatic efficiency ($T_{ce\lambda}$) of the resonance cell (D2 line). stem temperatures: 130, 138, 146, 155, 163, 174 °C (head: 190 °C)

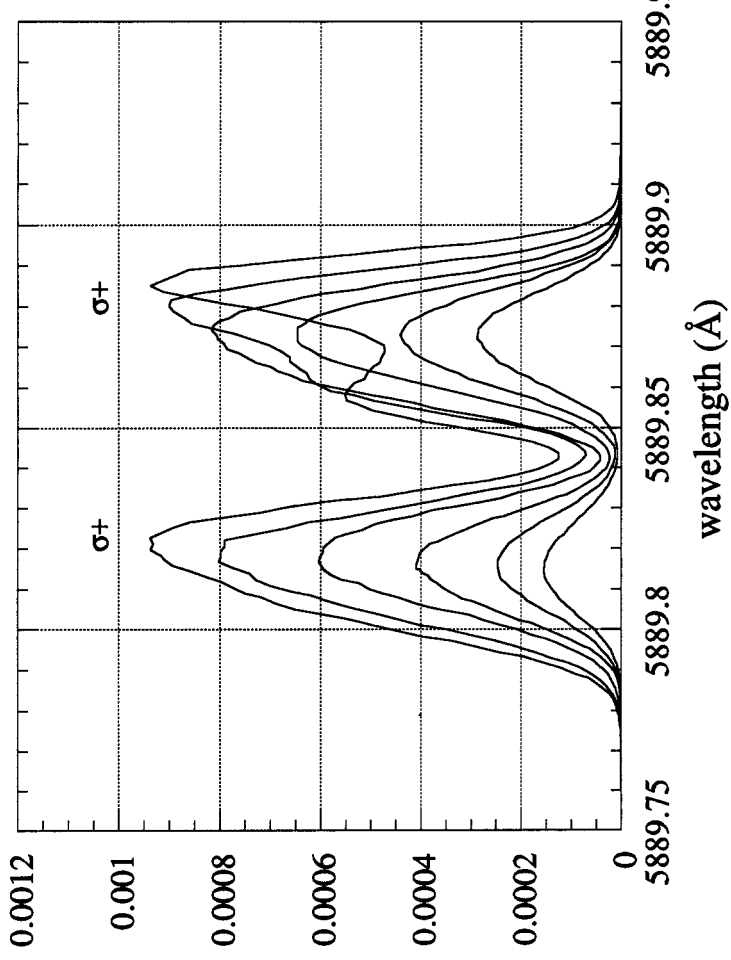

Figure 8: details of the monochromatic efficiency ($T_{ce\lambda}$) of the D2 line σ^+ components. stem temperatures: 130, 138, 146, 155, 163, 174 °C (head: 190 °C)

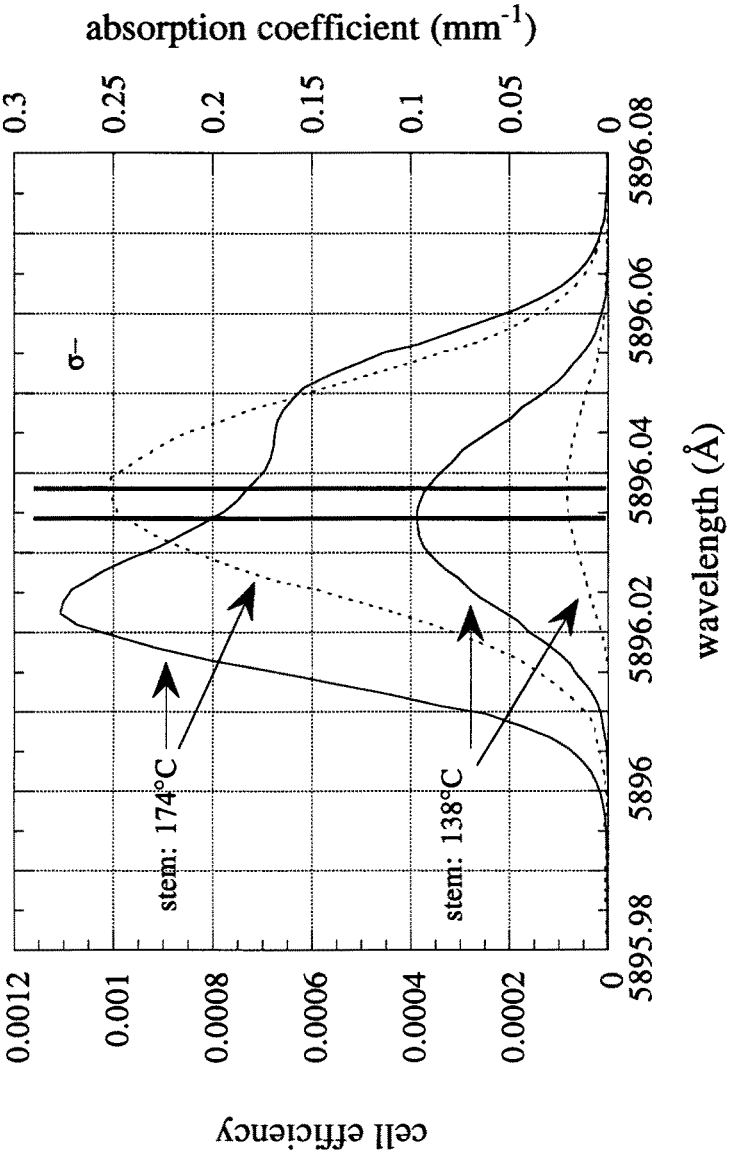

Figure 9: measured monochromatic efficiency ($T_{ce\lambda}$) of the cell (_____) and absorption coefficient derived from the transmission signal (- - - - -), for one σ^- component and two stem temperatures (D1 line).

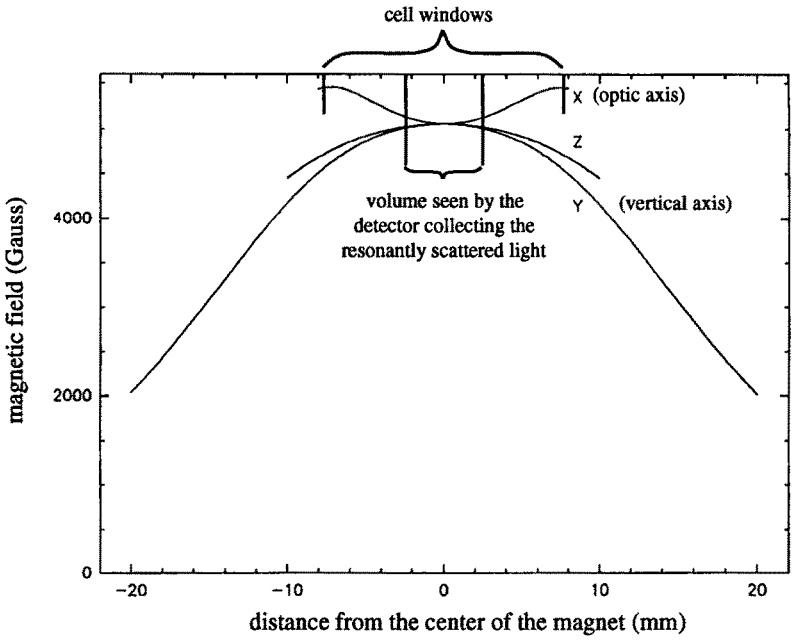

Figure 10: spatial distribution of the magnetic field in the cell

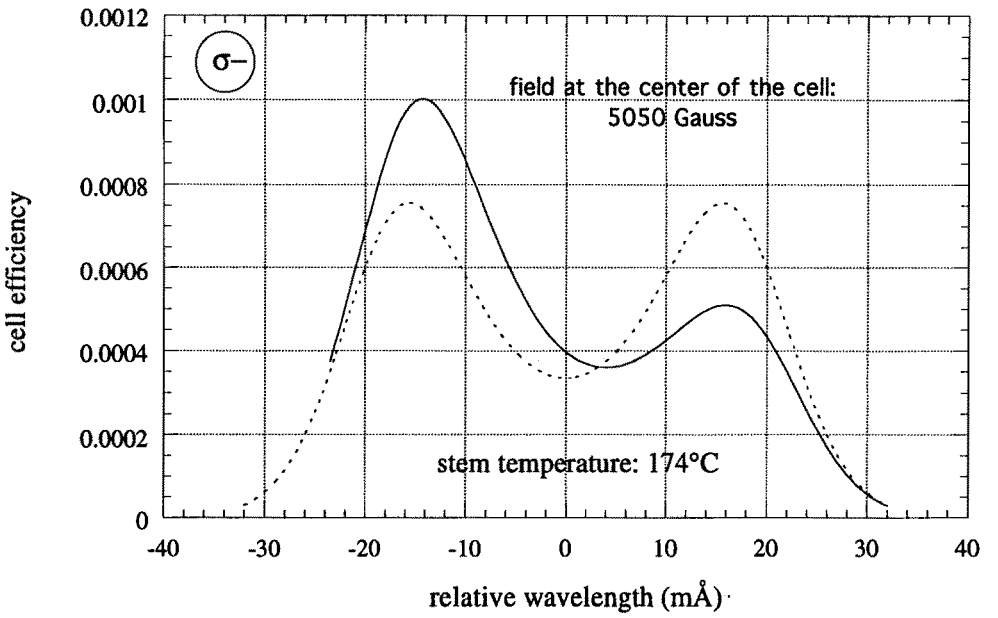

Figure 11: monochromatic efficiency ($T_{ce\,\lambda}$) of the cell calculated by the resonance model for one σ^-component (D1 line): (-----): with an homogeneous magnetic field in the vapour, (_____): with a realistic field gradient.

V CONCLUSION

The measurements we performed on a GOLF resonance cell prototype agree very well with the predictions of numerical simulations. The global fraction of light which reaches the detector through resonance processes is the one required to reach the nominal GOLF counting rate, i.e. to reach the desired sensitivity. The monochromatic profiles of the resonantly scattered light show the expected thermal properties. The saturation effect which reflects the equilibrium between the absorption and the re-emission in the vapour, is well demonstrated in the model and in the measurements. The heterogeneity of the magnetic field in the vapour creates an asymmetry of the saturated profiles, which could be used to design an optimal resonance system.

ACKNOWLEDGEMENTS

P. Boumier would like to thank the French National Space Center (C.N.E.S.) for the post-doctoral position and A.R. Jones the I.A.S. for the Poste Rouge position, that allowed them to perform the work detailed in this paper. This work would not have been possible without the contributions of many people of the I.A.S., especially of the Station d'étalonnage. All of them we sincerely and gratefully acknowledge.

REFERENCES

P. Boumier, Thèse de Doctorat de l'Université de Paris VII **(1991)**

P. Boumier and L. Damé, "GOLF: a resonance spectrometer for the observation of Solar Oscillations: I) Numerical model of the sodium cell response", accepted by Experimental Astronomy **(1993)**

J.R. Brookes, G.R. Isaak and H.B. van der Raay, Month. Not. Roy. Ast. Soc. 185, p. 1 **(1978)**

L. Damé, C. Cesarsky, P. Delache, F.L. Deubner, B. Foing, E. Fossat, C. Fröhlich, A. Gabriel, M. Gorisse, D. Gough, G. Grec, P.L. Pallé, J. Paul, T. Roca Cortés and J.L. Stenflo, "Global Oscillations at low frequencies (GOLF), an investigation of the Solar Interior", Proposal submitted to ESA and NASA in response to the Announcement of Opportunity SCI (87) 1/OSSA-1-87 for the Solar and Heliospheric Observatory, **(1987)**

E. Fossat and F. Roddier, Solar Phys. 18, p. 204, **(1971)**

JJ. Fourmond, Thèse de Doctorat de l'Université de Paris XI **(1992)**

C. Fröhlich, R.M Bonnet, A.V. Bruns, J.P. Delaboudinière, V. Domingo, V.A. Kotov, Z. Kollath, D.N. Rashkovsky, T. Toutain J.C. Vial, and Ch. Wehrli, in Proc. Symp. Seismology of the Sun and Sun-like Stars, ESA SP-286, p. 359, **(1988a)**

C. Fröhlich, B.N. Andersen, G. Berthomieu, P. Delache, V. Domingo, A.R. Jones, A. Jiménez, T. Roca Cortés and Ch. Wehrli, VIRGO : The Solar Monitor Experiment on SOHO, in Proc. Symp. Seismology of the Sun and Sun-like Stars, ESA SP-286, p. 371, **(1988b)**

C. Fröhlich, T. Toutain and C.J. Schriver, Helioseismology with the IPHIR instrument on the U.S.S.R PHOBOS Mission, Proceedings of Symposium ME7 of the COSPAR, Advances in space Research, **(1991)**

A.H. Gabriel and the GOLF team, Proceedings of Symposium ME7 of the COSPAR, Advances in space Research, vol. 11, p. 103 **(1991)**

Handbook of Chemistry and Physics, 64th. edition, CRC press. **(1983-1984)**

J.M. Robillot, R. Bocchia and N. Denis, The MR5 resonance spectrometer, I.R.I.S worshop, Marrakech, **(1991)**

P.H. Scherrer, J.T. Hoeksema and R.I. Bush, The Solar Oscillations Investigation - Michelson Doppler Imager for SOHO, Proceedings of Symposium ME7 of the COSPAR, Advances in space Research, **(1991)**

T. Toutain, and C. Fröhlich, A & A. 257, p. 287, **(1992)**

M. Woodard and H.S. Hudson, Nature 305, p. 589, **(1983)**

M. Woodard, Solar Phys. 114, p. 21, **(1987)**